

Structural Analysis of CaCO₃ Nanoparticle/Pulp Fiber Composites by Tube Flow Fractionation

Moe Fuchise-Fukuoka,^a Shisei Goto,^a and Akira Isogai^{b,*}

Two slurries that consisted of precipitated calcium carbonate (CaCO₃) nanoparticles and unbeaten hardwood bleached kraft pulp (HBKP) were prepared *via* ultrafine bubble and mixing methods. In the ultrafine bubble method, a CO₂ gas flow was bubbled into a HBKP slurry that contained Ca(OH)₂ to prepare a precipitated CaCO₃/HBKP composite slurry. The HBKP/water and precipitated CaCO₃/water slurries were prepared separately and mixed to prepare a precipitated CaCO₃/HBKP mixture slurry. Each of the two CaCO₃/HBKP slurries was separated into five fractions using a tube flow fractionation (TFF) system. The first and second fractions consisted of long HBKP fibers and fiber aggregates. The third fraction had the highest mass ratio of the components in the five fractions, and it had approximately 1-mm-long HBKP fibers. The fourth fraction contained primarily HBKP short fibers and CaCO₃ aggregates. Thus, the CaCO₃/HBKP components in the slurry were separated adequately by TFF, depending on their hydrodynamic sizes. The average width of each fraction in the CaCO₃/HBKP composite slurry was always larger than that of the corresponding fraction from the CaCO₃/HBKP mixture slurry, which indicated that precipitated CaCO₃ nanoparticles and their aggregates attached stably to long and short pulp fiber surfaces in the composite slurry.

Keywords: Classification; Nanoparticle; Precipitated calcium carbonate; Ultrafine bubble; Tube flow fractionation

Contact information: a: NPi Research Laboratory, Nippon Paper Industries Co., Ltd., 4-21-1 Oji, Kita-ku, Tokyo 114-0002, Japan; b: Department of Biomaterial Sciences, The University of Tokyo, 1-1-1 Yayoi, Bunkyo-ku, Tokyo 113-8657, Japan; *Corresponding author: aisogai@mail.ecc.u-tokyo.ac.jp

INTRODUCTION

Ground and precipitated calcium carbonate (CaCO₃) fillers are used as internal additives in alkaline papermaking to improve the optical and printing properties of paper. As the size, size distribution, and morphology of primary and secondary CaCO₃ particles can be controlled during precipitated CaCO₃ production to improve the filler retention, papermaking runnability, and resultant optical/printing properties of CaCO₃-filled paper, the use of precipitated CaCO₃ fillers as internal additives has dominated practical alkaline papermaking. When primary particles of precipitated CaCO₃ have nanosized structures, a portion of the CaCO₃ nanoparticles can interact physically with pulp fiber surfaces in paper stock (Kharisov and Kharissova 2010; Shen *et al.* 2010; Nypelö *et al.* 2012; El-Sherbiny *et al.* 2015; Julkapli and Bagheri 2015; Xia *et al.* 2015; Samyn *et al.* 2017; Jimoh *et al.* 2018). Therefore, it is important to clarify the interactions between long and short pulp fibers with precipitated CaCO₃ nanoparticles in paper stock to improve papermaking runnability and CaCO₃-filled paper quality.

Scanning electron microscopy (SEM) is useful to observe precipitated CaCO₃/pulp

fiber interactions at high magnification levels. However, it is difficult to determine whether the observed SEM images are representative of the target sample. Therefore, SEM can be used for qualitative studies, but it is inadequate for the quantitative characterization of CaCO₃/pulp fiber interactions. The classification of long and short pulp fibers in pulp slurries according to their sizes can be performed with a standard Bauer-pulp classifier with four tanks and metal slits that differ in size. The classifier is commercially available (Techlab Systems 2019). However, the classification of long and short fibers and fines in pulp slurries with the Bauer-pulp classifier is time-consuming and requires a large amount of pulp slurry with running water.

The tube flow fractionation (TFF) system was developed by Valmet Co. (Finland) for the efficient classification of long and short pulp fibers and fines according to their hydrodynamic sizes (Laitinen 2011). The principle of TFF classification has been reported in detail elsewhere (Laitinen 2011; Laitinen *et al.* 2011; Jagiello *et al.* 2016; Karinkanta and Laitinen 2017). Based on the TFF principle, an approximately 50 mL slurry that contained long and short fibers and fines was quickly separated into five fractions according to the hydrodynamic size of the components. The TFF system has been applied to various pulp fibers, recycled pulp fibers with residual inks, and wood powders to separate the components according to their hydrodynamic sizes (Laitinen 2011; Laitinen *et al.* 2011; Fukuoka *et al.* 2015a, 2015b; Jagiello *et al.* 2016; Karinkanta and Laitinen 2017). Fukuoka *et al.* (2015b) studied the distributions of residual ink particles in recycled pulp fibers and hydrophobic colloidal substances by TFF. Optical photographs in fractionated pulp slurries can be captured during the TFF classification by a charge-coupled device (CCD) camera, and the sizes and morphologies of the components and their agglomeration or aggregation behavior in each fraction can be analyzed qualitatively and quantitatively by image analysis.

In previous papers, new procedures were developed to prepare precipitated CaCO₃ nanoparticles or pulp-fiber composites using cavitation flow and ultrafine bubble methods to improve the adsorption stability of CaCO₃ nanoparticles on pulp fiber surfaces (Fukuoka *et al.* 2019; Fuchise-Fukuoka *et al.* 2020). In this study, a precipitated CaCO₃ nanoparticle or unbeaten pulp fiber slurry was separated into five fractions using TFF, and the interactions between the CaCO₃ nanoparticles and long and short pulp fibers were studied from optical and SEM images, mass ratios, and the CaCO₃ contents of the fractions. An unbeaten hardwood bleached kraft pulp (HBKP) was used, and two CaCO₃/HBKP slurries were used for TFF classification. One slurry was a CaCO₃/HBKP composite slurry that was prepared by flowing CO₂ gas into a HBKP slurry that contained Ca(OH)₂ *via* the ultrafine bubble method (Fuchise-Fukuoka *et al.* 2020). The other slurry was a CaCO₃/HBKP mixture slurry that was prepared by mixing HBKP/water and precipitated CaCO₃/water slurries that had been prepared separately.

EXPERIMENTAL

Preparation of Precipitated CaCO₃/Pulp Slurries

Never-dried HBKP (Nippon Paper Ind. Co., Ltd. Tokyo, Japan) was used without beating. Calcium hydroxide (Tama-ace U, Okutama Kogyo Co., Ltd., Tachikawa, Japan) was used without further purification. The CO₂ gas was prepared from commercial industrial-grade liquid CO₂ and held in a pressure-resistant cylinder. The precipitated CaCO₃ nanoparticle/HBKP composite was prepared from a 1 wt% HBKP/water slurry that

contained $\text{Ca}(\text{OH})_2$ (1 wt%) by blowing CO_2 gas with the ultrafine bubble method (Fuchise-Fukuoka *et al.* 2020). The dry mass ratio of the precipitated CaCO_3 :HBKP was set to 57:43 in the composite. The solid content of the composite slurry was diluted to 0.25% with water before being subjected to TFF. The CaCO_3 nanoparticles were prepared by bubbling CO_2 gas into a $\text{Ca}(\text{OH})_2$ solution without HBKP, and the CaCO_3 /HBKP mixture was prepared by mixing the precipitated CaCO_3 /water and the HBKP/water slurries (Fuchise-Fukuoka *et al.* 2020). The dry mass ratio of the precipitated CaCO_3 :HBKP and the solid content of the mixture slurry were set equal to those of the CaCO_3 /HBKP composite slurry.

TFF Classification

The TFF apparatus was a commercial product developed by Valmet Co. (Espoo, Finland) (Fig. 1). The CaCO_3 /HBKP composite or mixture slurry was separated into five fractions (Fr. #1, Fr. #2, Fr. #3, Fr. #4, and Fr. #5) by TFF (Fig. 2). Tables 1 and 2 show the experimental conditions. Photographs that corresponded to the five fractions were taken by using a charge coupled device (CCD) camera. The average fiber width in each fraction was determined from photographs using the Valmet IMG software (Ver. IMG75467, Valmet, Espoo, Finland) (Laitinen 2011; Laitinen *et al.* 2011; Fukuoka *et al.* 2015a, 2015b; Jagiello *et al.* 2016; Karinkanta and Laitinen 2017). The fractionation experiments were performed four times for each sample.

Analyses

Each fraction was collected and filtered using filter paper to collect the HBKP long and short fibers and CaCO_3 particles, and the dry mass of the solid components was determined by drying with the filter paper (Fuchise-Fukuoka *et al.* 2020). Part of the fraction sample was observed *via* a field-emission-type SEM (JSM-6700; JEOL, Tokyo, Japan) at 5 kV after coating with osmium *via* an OPC60A osmium plasma coater (Filgen, Japan). The CaCO_3 content of the solid component in each fraction was determined according to the standard incineration method JIS P 8251 (2003).

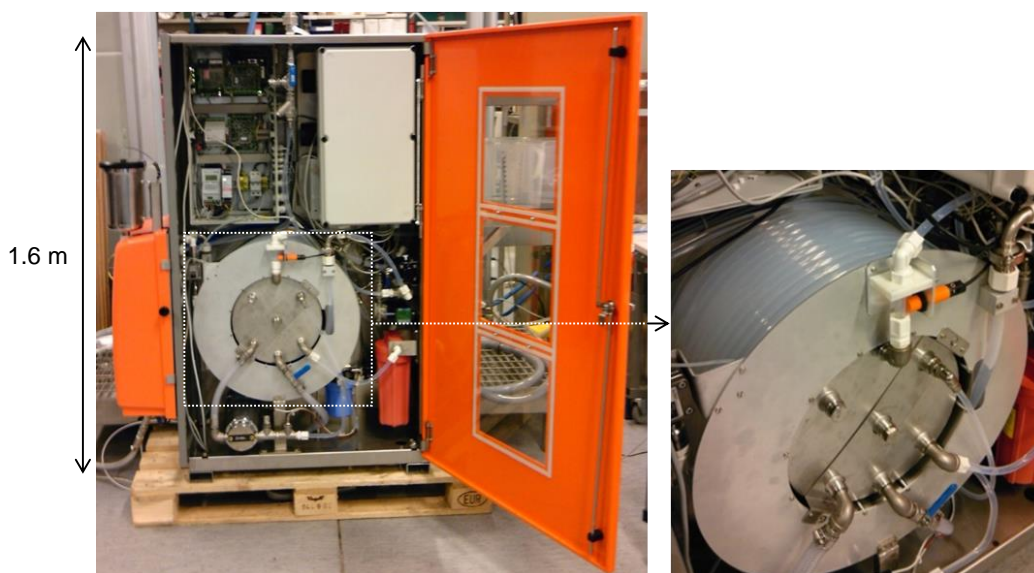


Fig. 1. Image of the Valmet tube flow fractionator (TFF)

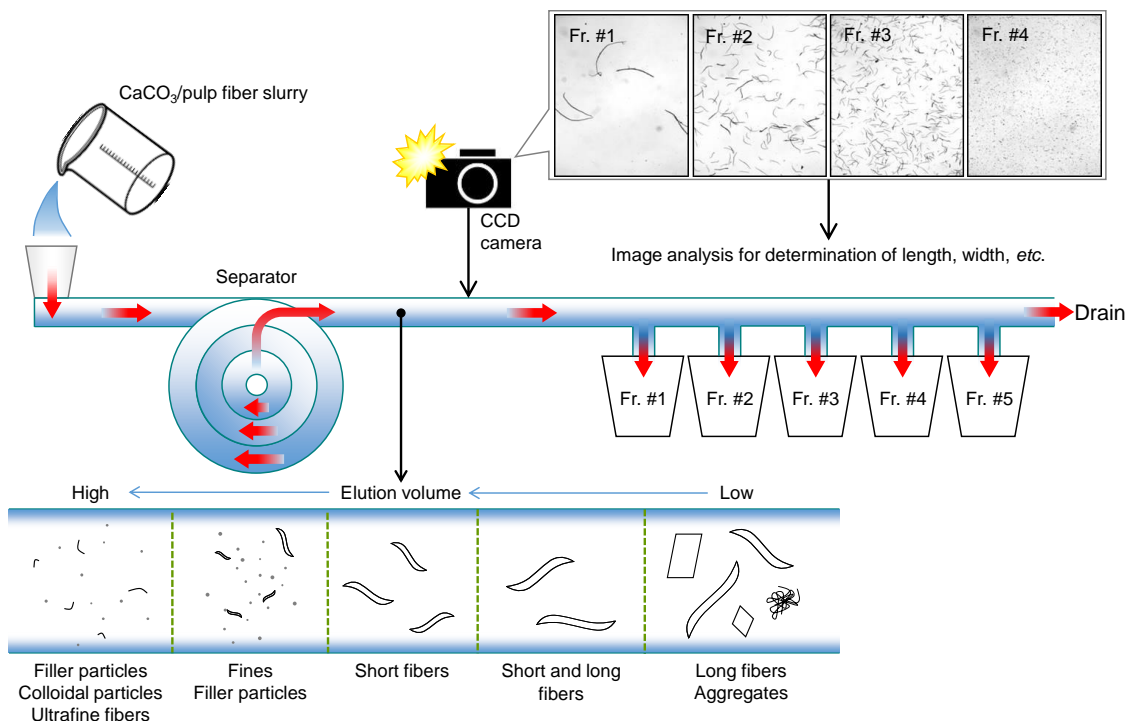


Fig. 2. Classification of $\text{CaCO}_3/\text{HBKP}$ slurry into five fractions using TFF (Fukuoka *et al.* 2015a, 2015b; Laitinen 2011; Laitinen *et al.* 2011; Jagiello *et al.* 2016)

Table 1. The Experimental Conditions of TFF

Water Temperature	25 °C to 26 °C	Inner Diameter of Fractionation Tube	16 mm
Flow Velocity	5.7 L/min	Length of Fractionation Tube	100 m
Initial Sample Consistency	0.25%	Reynolds Number	~ 8500
Sample Volume	50 mL		

Table 2. The TFF Classification Conditions

Fraction No.	Elution Time (s)	Elution Volume (L)
Fraction #1	10.6 to 27.2	16.00 to 17.55
Fraction #2	27.3 to 32.5	17.56 to 18.05
Fraction #3	32.6 to 37.3	18.06 to 18.50
Fraction #4	37.0 to 48.0	18.51 to 19.50
Fraction #5	48.1 to 59.0	19.51 to 20.50

RESULTS AND DISCUSSION

Fractionation of $\text{CaCO}_3/\text{HBKP}$ Composite and Mixture Slurries Using TFF

Based on the results obtained in preliminary experiments, the analytical conditions of TFF shown in Tables 1 and 2 were selected. Representative photographs of five fractions that were separated from the $\text{CaCO}_3/\text{HBKP}$ composite and mixture slurries by TFF under the conditions in Tables 1 and 2 are shown in Fig. 3. Fractions #1 and #2 consisted of

HBKP fibers and fiber aggregates. Individual HBKP fibers of approximately 1 mm in length were present in Fr. #3. Fraction #4 consisted of short fibers and CaCO₃ aggregates, and Fr. #5 had fine CaCO₃ particles and likely had ultrafine fibers. These images suggest that the components in both slurries were adequately separated into five fractions by TFF according to the hydrodynamic size of the components.

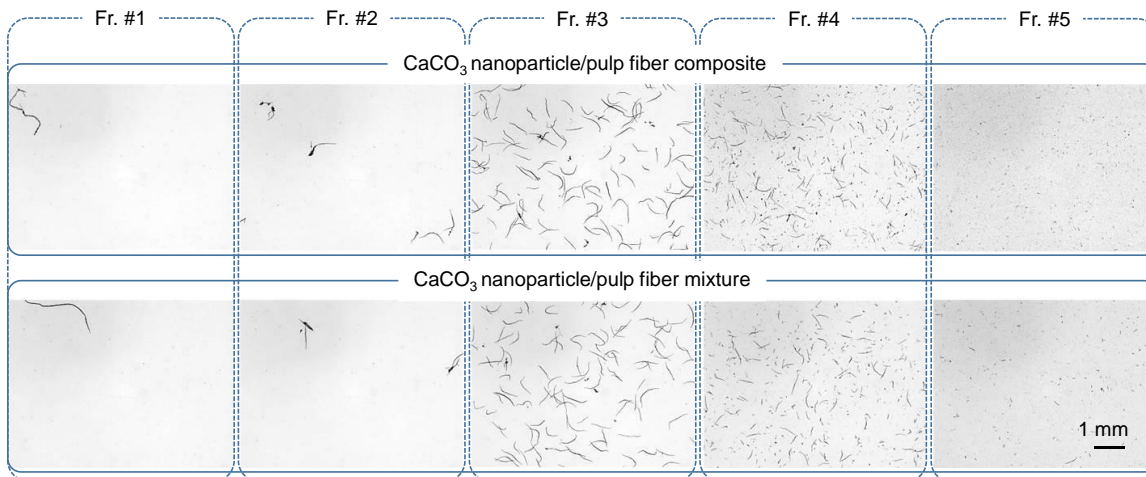


Fig. 3. Photographs of the fractions separated from the CaCO₃/HBKP composite and mixture slurries by TFF (taken with a CCD camera)

Laitinen (2011) and Laitinen *et al.* (2011) reported that pulp slurries were separated into fractions according to fiber length (rather than fiber width) by TFF. The average width of the components in each fraction was determined from multiple photographs (Fig. 3) with the Valmet IMG software (Fig. 4). For the two slurries, the average fiber widths decreased as fraction number increased. The average fiber widths of Fr. #1 and Fr. #2 of the CaCO₃/HBKP composite slurry, which consisted primarily of HBKP fibers and fiber aggregates, were larger than those in the corresponding fractions of the mixture slurry. The difference in the average fiber widths of Fr. #3 and Fr. #4 was small between the composite and mixture slurries. However, the average fiber widths of Fr. #3 and #4 were different for the composite and mixture slurries.

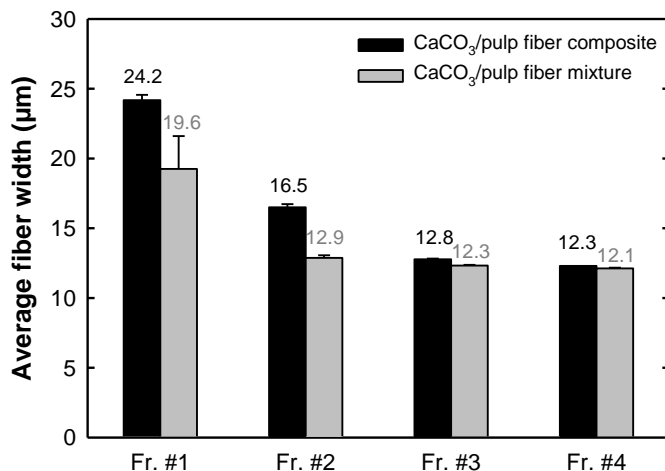


Fig. 4. The average fiber width of each fraction separated from CaCO₃/HBKP composite and mixture slurries by TFF

Therefore, the average fiber width in each fraction for the CaCO₃/HBKP composite slurry was always larger than that for the CaCO₃/HBKP mixture slurry. This likely occurred because large amounts of CaCO₃ nanoparticles were attached stably to long and short fiber surfaces. Because the average fiber width of HBKP and its freeness were unchanged before and after soaking in 1% Ca(OH)₂ solution, the Ca(OH)₂ treatment did not influence the HBKP morphology and freeness (Fuchise-Fukuoka *et al.* 2020).

SEM Observation of Fractions

The representative SEM images of the fractions for the CaCO₃/HBKP composite and mixture slurries are shown in Fig. 5. The CaCO₃ nanoparticles covered the HBKP fiber surfaces in Fr. #1C to Fr. #4C for the CaCO₃/HBKP composite. In contrast, few CaCO₃ nanoparticles were observed on the HBKP long and short fiber surfaces in Fr. #1M to Fr. #4M for the CaCO₃/HBKP mixture. In the SEM images of Frs. #1C to #4C in Fig. 5, the CaCO₃ nanoparticles and HBKP long and short fibers formed large aggregates, which indicated that the CaCO₃ nanoparticles on the HBKP long and short fiber surfaces bonded with other CaCO₃ nanoparticle-attaching HBKP long and short fibers. Therefore, the characteristic SEM images for the CaCO₃/HBKP composite, which differ from those of the CaCO₃/HBKP mixture, were caused by the presence of CaCO₃ nanoparticles that were attached stably on the HBKP long and short fiber surfaces prepared *via* the ultrafine bubble method (Fuchise *et al.* 2019).

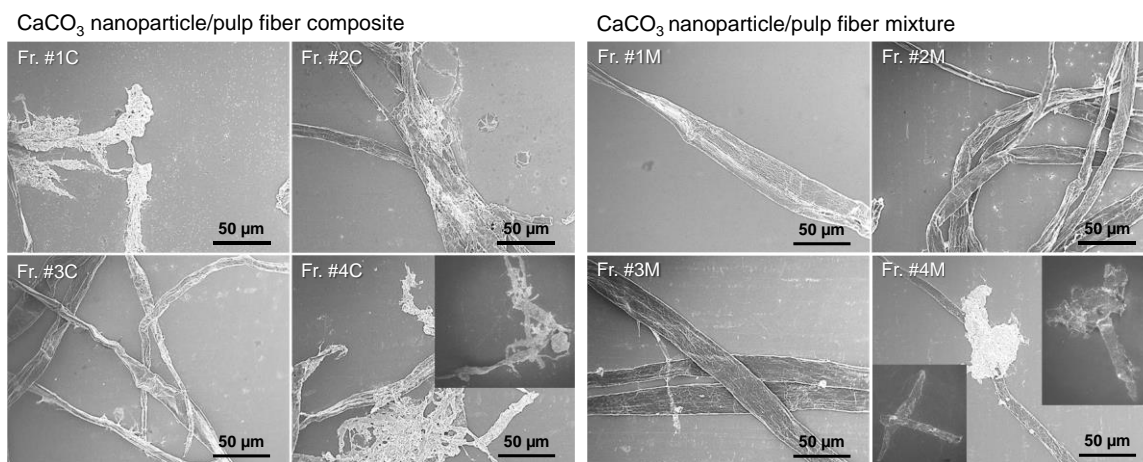


Fig. 5. The SEM images of fractions separated from the CaCO₃/HBKP composite (Fr. #1C to Fr. #4C) and CaCO₃/HBKP fiber mixture (Fr. #1M to Fr. #4M) by TFF

Dry Mass of Solid Components in Each Fraction

The dry masses of the solid components in each fraction were determined by filtration using filter paper and drying of the filtered residue (Fig. 6). The two slurries had similar mass distributions of solid components between the five fractions; the solid mass values were in the order of Fr. #4 > Fr. #3 > Fr. #5 > Fr. #2 > Fr. #1. The total masses of solid components from Fr. #1 to Fr. #5 for the CaCO₃/HBKP composite and mixture slurries were 88.5 mg and 78.7 mg, respectively, which were lower than that of the solid components (125 mg) that were present originally in the slurries. This result indicated that part of the precipitated CaCO₃ nanoparticles that was not attached to the HBKP long or short fibers filtered through the filter paper and was lost as filtrate.

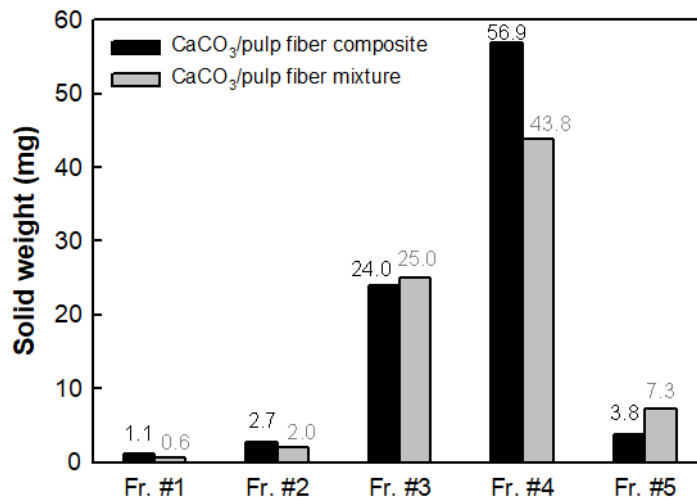


Fig. 6. The dry masses of the solid components in each fraction separated from CaCO₃/HBKP composite and mixture slurries by TFF

Because the mass of solid components in Fr. #4 for the composite slurry was higher than that for the mixture slurry, a higher amount of CaCO₃ nanoparticles and/or HBKP short fibers was present in Fr. #4 for the composite slurry than for the mixture slurry. Although the absolute dry masses of Fr. #1 and Fr. #2 were low, the composite slurry had higher solid masses than the mixture slurry, which indicated that the CaCO₃ nanoparticles attached stably to the HBKP fibers prepared with the ultrafine bubble method, and their presence in the composite slurry caused these results.

The dry solid mass in Fr. #3 for the composite slurry was slightly lower than that for the mixture slurry. This likely occurred because part of the HBKP fibers that were originally present in Fr. #3 aggregated with CaCO₃ nanoparticles to move Fr. #1 or Fr. #2. Consequently, the dry solid masses in Frs. #1 and #2 for the composite slurry were higher than those for the mixture slurry. The dry solid mass in Fr. #5 for the composite slurry was lower than that for the mixture slurry, which probably occurred because CaCO₃ nanoparticles that did not form aggregates with HBKP short fibers were present preferentially in this fraction of the mixture slurry.

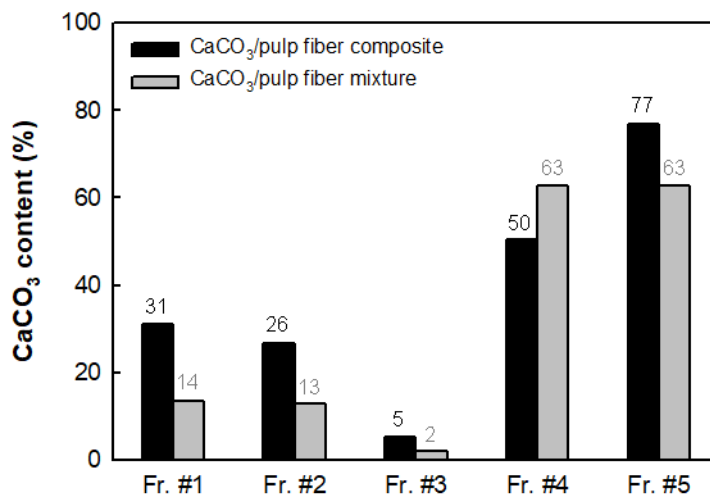


Fig. 7. The CaCO₃ contents of the solid components present in the fractions separated from CaCO₃/HBKP fiber composite and mixture by TFF

CaCO₃ Content of Composite and Mixture Components

The CaCO₃ content of each fraction was determined *via* the standard incineration method (Fig. 7). The CaCO₃ contents in Fr. #1 to Fr. #3 of the CaCO₃/HBKP composite were more than twice those of the CaCO₃/HBKP mixture. Therefore, the CaCO₃ nanoparticles attached stably to the HBKP fibers when the ultrafine bubble method of the CO₂ gas was used in composite sample preparation. The high CaCO₃ contents of Fr. #1 to Fr. #3 in the composite slurry were consistent with those in Fig. 4; the fiber widths in the composite slurry were higher than those in the mixture slurry. The results in Fig. 7 were in accordance with those of the SEM images in Fig. 5; the CaCO₃ nanoparticles attached stably to HBKP fiber surfaces in the CaCO₃/HBKP composite.

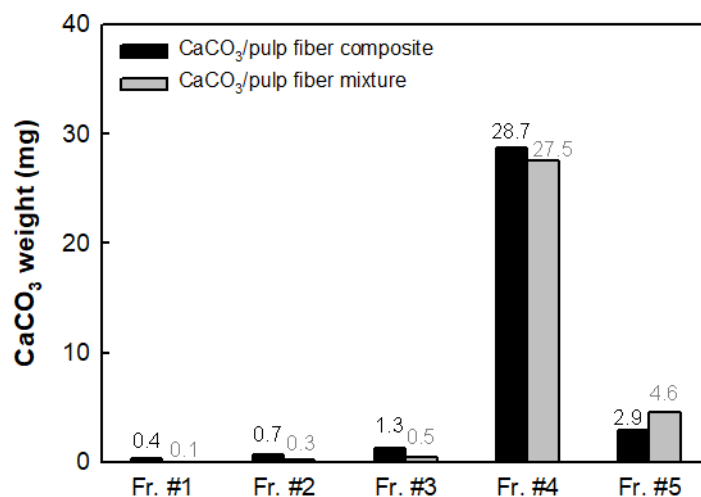


Fig. 8. CaCO₃ mass in each fraction calculated from results in Figs. 6 and 7

The masses of CaCO₃ in each fraction were calculated from the results in Figs. 6 and 7, and they are shown in Fig. 8. Because most precipitated CaCO₃ particle aggregates and short fiber/CaCO₃ aggregates were present in Fr. #4, it had the highest mass of CaCO₃. The masses of CaCO₃ in Fr. #1 to Fr. #4 for the composite slurry were higher than those for the mixture slurry, which was consistent with the results in Fig. 4 and Fig. 5. The CaCO₃ nanoparticles and their aggregates attached stably to HBKP long and short fibers in the composite slurry.

Versatile inorganic nanoparticle/pulp fiber composites can be prepared by the ultrafine bubble method, as shown in this study, at the industrial level for production of specialty papers with high values such as deodorant, anti-bacterial, flame-retardant, and X-ray shielding properties. The results obtained in this study showed that the TFF method is applicable to characterization of the inorganic nanoparticle/pulp fiber composites at the slurry stages in short times and to feedback of the obtained results to the production process.

CONCLUSIONS

1. The CaCO₃/HBKP composite or mixture slurry was separated into five fractions according to the hydrodynamic size of the components by TFF. The HBKP fiber aggregates, long and short fibers with or without aggregates of CaCO₃ nanoparticles, and CaCO₃ nanoparticles and their aggregates were adequately separated according to

their hydrodynamic sizes by TFF under the selected conditions.

2. The average fiber width in each fraction was measured from photographs using an image analyzer. Because the CaCO₃ nanoparticles attached stably to the HBKP long and short fibers, the average fiber widths in Fr. #1 to Fr. #4 for the composite slurry were larger than those for the mixture slurry. This result was supported by the SEM images of each fraction; the HBKP long and short fibers in the composite slurry were present with aggregates of CaCO₃ nanoparticles, whereas those in the mixture slurry were not.
3. The TFF classification method can be used to precipitate CaCO₃ nanoparticle/HBKP composite and mixture slurries for structural analyses of the components separated and present in each fraction.

ACKNOWLEDGEMENTS

The authors thank Mr. Kazuhiro Kurosu, Mr. Dai Nagahara, Mr. Susumu Kato, Mr. Masatoshi Oishi, Takuya Okawa of Nippon Paper Industries, and Dr. Keita Fuchise of the National Institute of Advanced Industrial Science and Technology (AIST) of Japan for their support.

REFERENCES CITED

- El-Sherbiny, S., El-Sheikh, S. M., and Barhoum, A. (2015). "Preparation and modification of nano calcium carbonate filler from waste marble dust and commercial limestone for papermaking wet end application," *Powder Technol.* 279, 290-300. DOI: 10.1016/j.powtec.2015.04.006
- Fukuoka, M., Goto, S., and Ohtake, H. (2015a). "Novel analysis method for pulp furnish using tube flow fractionator (Part 1)," *Japan TAPPI J.* 69(4), 432-437. DOI: 10.2524/jtappij.69.432
- Fukuoka, M., Suzuki, H., Nakatani, T., and Goto, S. (2015b). "Novel analysis method for pulp furnish using tube flow fractionator (Part 2)," *Japan TAPPI J.* 69(9), 987-993. DOI: 10.2524/jtappij.69.987
- Fukuoka, M., Nakatani, T., and Goto, S. (2019). "Development of mineral hybrid fiber from calcium carbonate and pulp using fluid — jet cavitation," *Japan TAPPI J.* 73(11), 1103-1116. DOI: 10.2524/jtappij.73.1110
- Fuchise-Fukuoka, M., Oishi, M., Goto, S., and Isogai, A. (2020). "Preparation of CaCO₃ nanoparticle/pulp fiber composites with ultrafine bubbles," *Nord Pulp Pap. Res. J.* 35, 279-287. DOI: 10.1515/npprj-2019-0078
- Jagiello, L. A., Redlinger-Pohn, J. D., Fischer, W. J., Eckhart, R., and Bauer, W. (2016). "The effect of Dean flow in a tube flow fractionation device," *Nord. Pulp Pap. Res. J.* 31(4), 642-647. DOI: 10.3183/NPPRJ-2016-31-04-p641-647
- Jimoh, O. A., Ariffin, K. S., Hussin, H. B., and Temitope, A. E. (2018). "Synthesis of precipitated calcium carbonate: A review," *Carbonate Evaporite* 33, 331-349. DOI: 10.1007/s13146-017-0341-x
- JIS 8251 (2003). "Paper, board and pulps—Determination of residue (ash) on ignition at 525 degrees C," Japanese Industrial Standard Committee, Tokyo, Japan.

- Julkapli, N. M., and Bagheri, S. (2015). "Developments in nano-additives for paper industry," *J. Wood Sci.* 62, 117-130. DOI: 10.1007/s10086-015-1532-5
- Karinkanta, P., and Laitinen, O. (2017). "Use of tube flow fractionation in wood powder characterization," *Biomass Bioenerg.* 99, 122-138. DOI: 10.1016/j.biombioe.2017.02.011
- Kharisov, B. I., and Kharissova, O. V. (2010). "Advances in nanotechnology in paper processing," *Int. J. Green Nanotechnol: Mater. Sci. Eng.* 2(1), M1-M8. DOI: 10.1080/19430841.2010.488204
- Laitinen, O. (2011). *Utilisation of Tube Flow Fractionation in Fibre and Particle Analysis*, Doctoral Thesis, University of Oulu, Oulu, Finland.
- Laitinen, O. T., Kempainen, K., Stoor, T., and Niinimäki, J. (2011). "Fractionation of pulp and paper particles selectively by size," *BioResources* 6(1), 672-685. DOI: 10.15376/biores.6.1.672-685
- Nypelö, T., Pynnönen, H., Österberg, M., Paltakari, J., and Laine, J. (2012). "Interactions between inorganic nanoparticles and cellulose nanofibrils," *Cellulose* 19, 779-792. DOI: 10.1007/s10570-012-9656-x
- Techlab Systems (2019). "Bauer McNett fibre classifier," (https://techlabsystems.com/en/datasheets/pulp/cf_bauer_mcnett_fibre_classifier.pdf), Accessed 10 April 2020.
- Samyn, P., Barhoum, A., Öhlund, T., and Dufresne, A. (2017). "Review: Nanoparticles and nanostructured materials in papermaking," *J. Mater. Sci.* 53, 146-184. DOI: 10.1007/s10853-017-1525-4
- Shen, J., Song, Z., Qian, X., Yang, F., and Kong, F. (2010). "Nanofillers for papermaking wet end applications," *BioResources* 5(3), 1328-1331. DOI: 10.15376/biores.5.3.1328-1331
- Xia, C., Shi, S. Q., Cai, L., and Nasrazadani, S. (2015). "Increasing inorganic nanoparticle impregnation efficiency by external pressure for natural fibers," *Ind. Crop. Prod.* 69, 395-399. DOI: 10.1016/j.indcrop.2015.02.054

Article submitted: April 12, 2020; Peer review completed: June 4, 2020; Revised version received: June 15, 2020; Accepted: July 23, 2020; Published: July 28, 2020.
DOI: 10.15376/biores.15.3.7048-7057